

# Array Configuration for the Long Wavelength Intermediate Array (LWIA): Choosing the First Four Station Sites

Aaron Cohen (NRL) and Greg Taylor (UNM)

December 4, 2007

## ABSTRACT

The Long Wavelength Intermediate Array (LWIA) will consist of 16 LWA stations arranged with baselines from 1 to 200 km. This will be the first stage of the LWA that will be capable of routinely imaging sources with complex or extended structure. The array configuration of these 16 stations will be determined both from logistical constraints as well as to achieve the best possible imaging capability. Recently, preliminary site studies have been done on over 30 possible station sites throughout the southwest of New Mexico. We have identified all possible array configurations that can be produced from the sites that have been shown to be most promising. We have rated the imaging capability of each potential configuration by creating simulated images at various declinations for the large and complex source Cygnus A. We list the configurations that produce the highest image fidelity. From this, we have identified the best four sites to begin developing.

## 1. Introduction

The Long Wavelength Array (LWA) will eventually consist of 52 stations, with baselines up to 400 km (Cohen 2006). This will be built in stages according to the development plan described in Taylor et al. (2006a), and the first stage capable of routine imaging of complex sources will be the 16-station Long Wavelength Intermediate Array (LWIA-16). The LWIA-16 will consist of a 6-station core and 10 outlying stations with baselines up to 200 km. The construction of the first three stations is scheduled to begin within the next 1-2 years for the LWA1+ stage. Because site selection and acquisition are rather complicated and time-consuming processes, it is essential that this begin as soon as possible. As these first stations will be only the beginning of the eventual LWIA-16, they must be chosen so that they fit into a 16-station array that is optimized for the best possible imaging capability. Therefore we must now plan as well as possible the array design for the final LWIA-16, and from this choose the first three stations to construct.

In order to be prepared for the first three stations, we have chosen to begin development work on four sites so that there will be a “spare” if there is any unanticipated problem with one of the sites. One of these will be located in the LWA core on a site we call North Arm (NA). That leaves three sites to be chosen outside the core. The purpose of this report is to choose these first three outlier sites in the context of the best possible LWIA-16 array configuration.

We intend the LWIA-16 to operate as a real-time connected element interferometer over high-bandwidth fiber (Taylor et al. 2006a). Therefore, we have only considered site locations on or near existing commercial optical fiber lines. Work to secure access to these fiber lines is ongoing but unlikely to be finalized before site acquisition must begin to meet the LWA development schedule. However, Taylor (2007b) has shown that it would also be possible to operate the LWA via lower bandwidth links, bringing time-stamped data back over disks. That would serve as a “back-up” plan should the preferred option of a fiber-connected array prove impractical.

## 2. Array Optimization

There are many methods for optimizing arrays, and many different figures of merit used. One example is the side-lobe optimization technique developed by Leonia Kogan, and used for the LWA station design (Kogan and Cohen 2005), the VLA E-configuration and ALMA configuration studies. This technique uses an iterative process to rearrange the array elements to lower the side-lobes of the synthesized beam. While successful, this method relies on either complete or at least significant freedom of movement of the array elements. For example, within an LWA station, the antennas can be moved anywhere within a  $\sim 100$  meter diameter region.

This is not the case for the LWA array design. The positions of the stations cannot be varied continuously. Rather we must choose from a relatively small set of suitable locations. While optimization algorithms do not apply to such a problem, we still need to choose sites to maximize the imaging capability of the final array design. Fortunately, the discreet nature of this problem means that there are a finite number of possible array configurations. Once one decides on a figure of merit, the “best” of these finite options can be identified. This is the method we have used to determine the best LWIA array configurations.

## 3. Candidate Sites for LWA Stations

The LWA core will be placed near the north VLA arm, and six of the 16 LWIA stations will be placed in this region. For the 10 outlying stations, roughly 30 candidate sites have been identified based on various suitability factors including: land ownership, road access, existing optical fiber access, radio frequency interference (RFI) environment, and terrain. Exploratory visits to each of these sites have recently been completed (Taylor et al. 2006b, 2007a; Dickel et al. 2007) and 15 of these sites have been identified as the most promising in terms of both logistics and their potential to enhance the spatial frequency coverage of the final array. These 15 sites are listed in Table 1, and each of them have been named (ex: Horse Springs) and given a two-letter code (ex: HS) which is how they will be referenced for the remainder of this report. Along with the six core stations (including “North Arm” or NA), Figure 1 shows the locations of these 15 candidate sites, each labeled by its two-letter code.

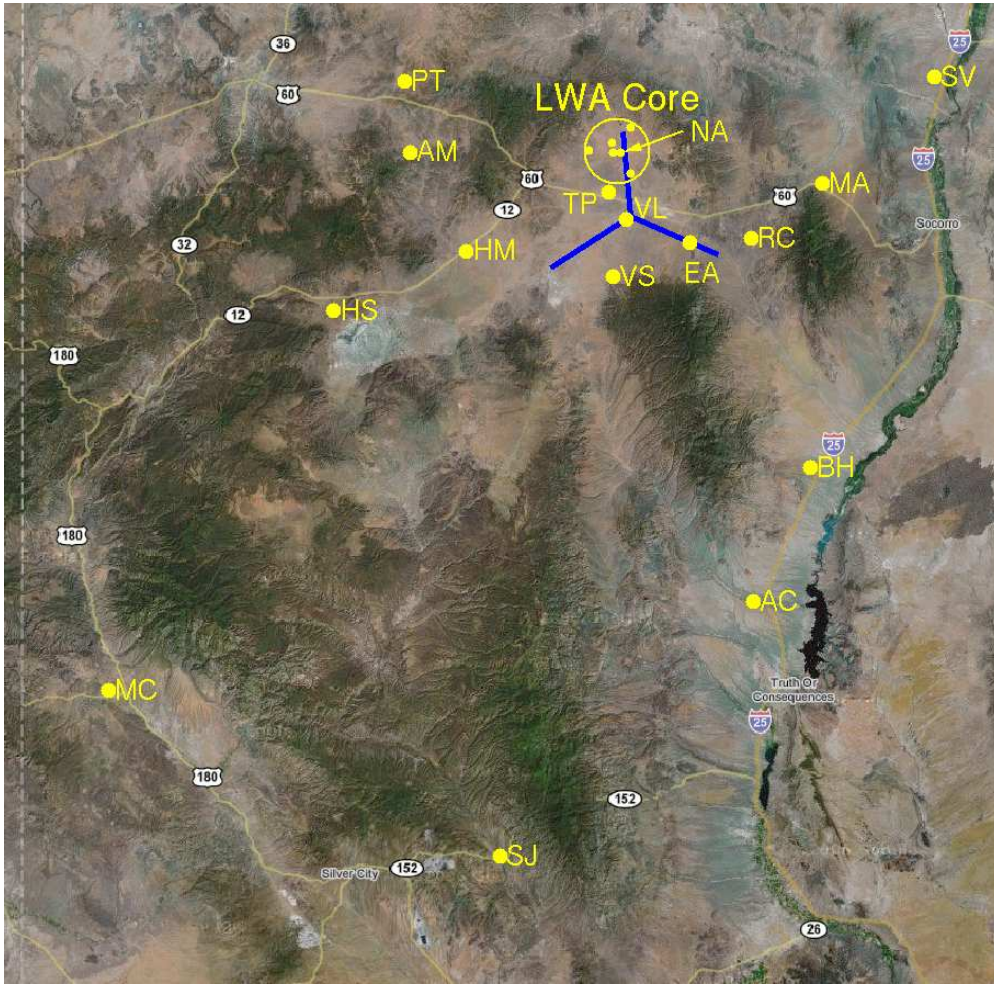


Fig. 1.— Candidate LWIA-16 station sites found to be suitable after visiting. Six stations will be in the LWIA core, including the NA site.

We already know the locations of the core stations which includes NA. For the 10 outlier sites, we must choose 10 of the 15 candidate outlier sites. With no constraints, there are 3,003 unique sets of 10 that can be chosen from 15 elements. However, this number can be reduced by applying some reasonable constraints. First, we know that the station VL, which is the site of the Long Wavelength Development Array (LWDA), will eventually become a site. So this can be fixed. Also, in order to achieve the desired resolution, we must have the long baselines to the core from the southwest, south and southeast directions provided by the MC, SJ and AC sites respectively. Fixing those as well, leaves a choice of 6 of the remaining 11. There are 462 such combinations, which is still large, but now a more reasonable amount to study. None of these four fixed sites can be used for the LWA1+ because MC, SJ and AC have baselines that are too long for this initial stage, and VL is currently occupied by the LWDA and other prototype antennas.

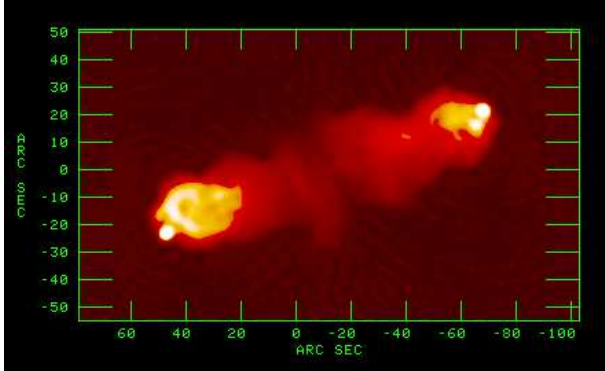


Fig. 2.— Cygnus A at 325 MHz imaged with the VLA in A-configuration with the Pie Town link. The resolution is  $2.5''$ .

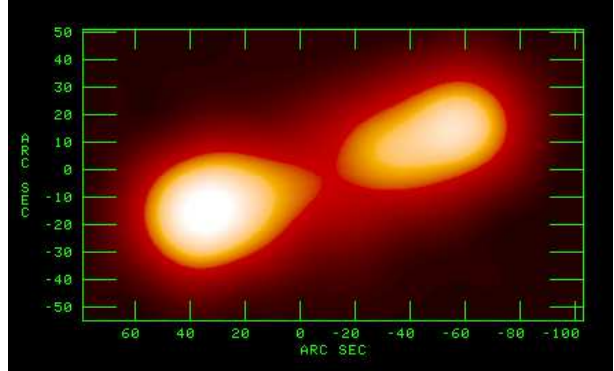


Fig. 3.— Cygnus A at 74 MHz imaged with the VLA in A-configuration.

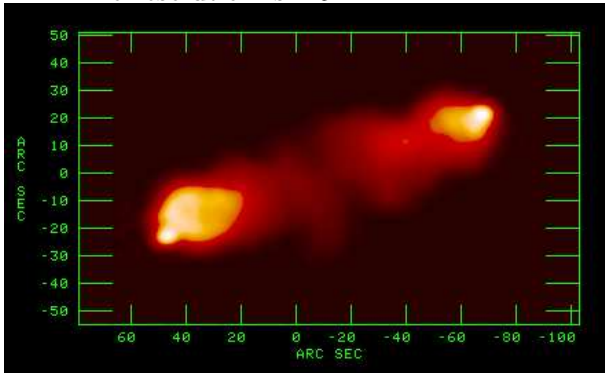


Fig. 4.— Simulated 74 MHz image of Cygnus A with one potential configuration of the LWIA-16.

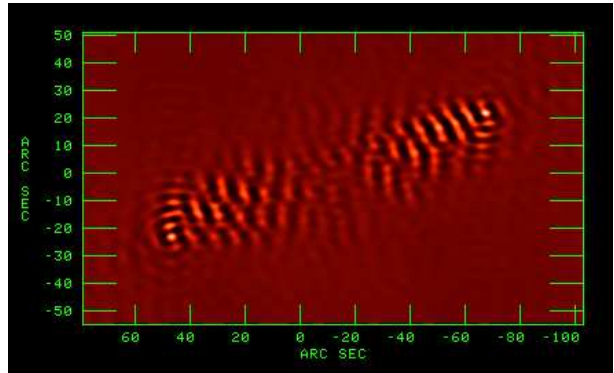


Fig. 5.— Residual image after subtracting from the simulated Cygnus A image the model image convolved to the same resolution.

#### 4. Image Fidelity

The natural figure of merit for potential array configurations is image fidelity, or the ability to accurately reconstruct the source structure of celestial radio sources. Image fidelity is best measured with image simulations of a source that has source structure typical of that which the instrument will need to map. For this purpose, we have used the source Cygnus A, shown at 325 MHz in Figure 2. Cygnus A is a reasonable choice because it contains both small-scale features and large-scale diffuse emission. The true high-resolution structure is not known at low frequencies ( $\leq 100$  MHz) because even the 74 MHz image taken with the largest VLA configuration has rather poor resolution (Figure 3). However, it is possible to use the higher frequency image as a model. Although the source morphology will certainly be somewhat different at 325 MHz than at lower frequencies, this model is sufficient for the purpose of image simulations.

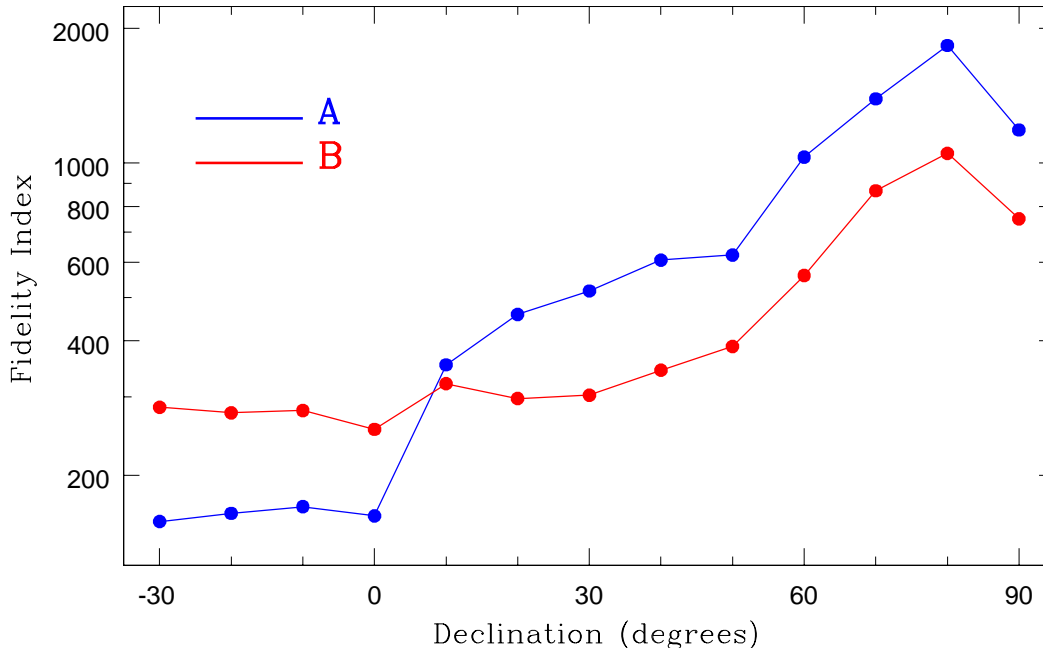


Fig. 6.— Fidelity index for two array options as a function of source declination.

For a given array configuration, the first step in image simulation is to create simulated visibility data. This is done with an algorithm written by Leonia Kogan (and implemented in AIPS as the task UVCON) that creates a database of visibilities calculated based on the source model, array geometry, frequency, simulated source location in the sky and hour-angle range of the observation. Next, this visibility data set is processed using the normal image processing algorithms used to create images from raw VLA data. This results in a simulated image, as seen in Figure 4 at 74 MHz for a sample LWIA configuration. Finally, the model image is convolved to the resolution of the simulated image and subtracted from the simulated image to create a residual map as shown in Figure 5. This residual map shows the inaccuracies in the image re-construction mainly due to incomplete spatial-frequency ( $uv$ ) coverage. A “fidelity index” can be defined as the ratio of the peak flux density in the model image to the RMS variations in the residual map. The higher the fidelity index, the better the image fidelity.

## 5. Simulating the LWIA-16

The LWIA-16 will not have the full imaging capability of the full 52-station LWA. Initially it will be limited to relatively bright and isolated sources (Cohen et al. 2007). Because of the limited spatial-frequency ( $uv$ ) coverage, snapshot imaging capability will still be very limited and most imaging of complex sources will need to be done with “full-track” observations. Therefore

the imaging we have simulated is for time-synthesis observations that last the entire time that a source is above  $20^\circ$  elevation. While the dipole beam pattern will be attenuated at the low end of this elevation limit, there will still be plenty of sensitivity for the relatively bright objects described in Cohen et al. (2007). We also note that these simulations make use of current software that uses a constant primary beam shape, yet the LWA primary beam will become elongated at lower elevations. However, this also is not a significant factor as the primary goal of the LWIA-16 will be to image bright isolated sources, and in such cases we only need to be concerned with the very center of the field of view.

We simulated sources located at each of the 13 declinations between  $-30^\circ$  to  $+90^\circ$  at  $10^\circ$  degree intervals. Figure 6 plots the resulting fidelity index for two potential arrays shown for comparison. In general, the fidelity index improves for higher source declinations, because earth-rotation synthesis is more effective at higher declinations and away from the equator. This is seen for both configurations shown. However, this difference is less dramatic for configuration “B”. So while configuration “A” has better image fidelity at high declinations, configuration “B” does not decline as much at the lower declinations. It is desirable for the LWIA to have high image fidelity over the entire sky, and to not have “holes” where its performance is very poor. Therefore, configuration “B” is preferable, because its worst values are higher than the worst values for configuration “A”. While configuration “A” performs better at high declinations, configuration “B” is better over the sky as a whole.

With this in mind, we use two parameters to evaluate each configuration. One is the minimum value of the fidelity index for each declination simulated. The second is the geometric mean of the fidelity index for all declinations weighted by the solid angle of sky at each declination (proportional to  $\cos \delta$ ). This is meant to reflect the overall performance, and we will refer to this as the “average” fidelity index. Figure 7 plots all 462 possible array configurations as a function of these two parameters. There is a clear correlation between the average and minimum fidelity indices, but many comparisons involve trade-offs between a configuration that has a better average fidelity index to one that has a better minimum fidelity index. Clearly both are important. For this reason, we have chosen the figure of merit (FOM) to be the geometric mean of the minimum and average fidelity indices. Also plotted in Figure 7 are contours of constant FOM, labeled as a percentage of the configuration with the highest FOM. By this standard, returning to the configurations compared in Figure 6, “B” has a significantly higher FOM than “A” (289.39 vs. 232.55).

## 6. Results and Discussion

Figure 7 demonstrates that none of the possible array configurations for the LWIA are dramatically better than all the rest. Rather, there is a roughly continuous spread of FOM values ranging from the highest value of 359.46 to the lowest value of 58.18. In fact, of the 462 configurations, 20 of them have a FOM at least 90% as high as the “best” configuration. This is good news, because if practical considerations make the “best” configuration impossible, or too expensive, there are

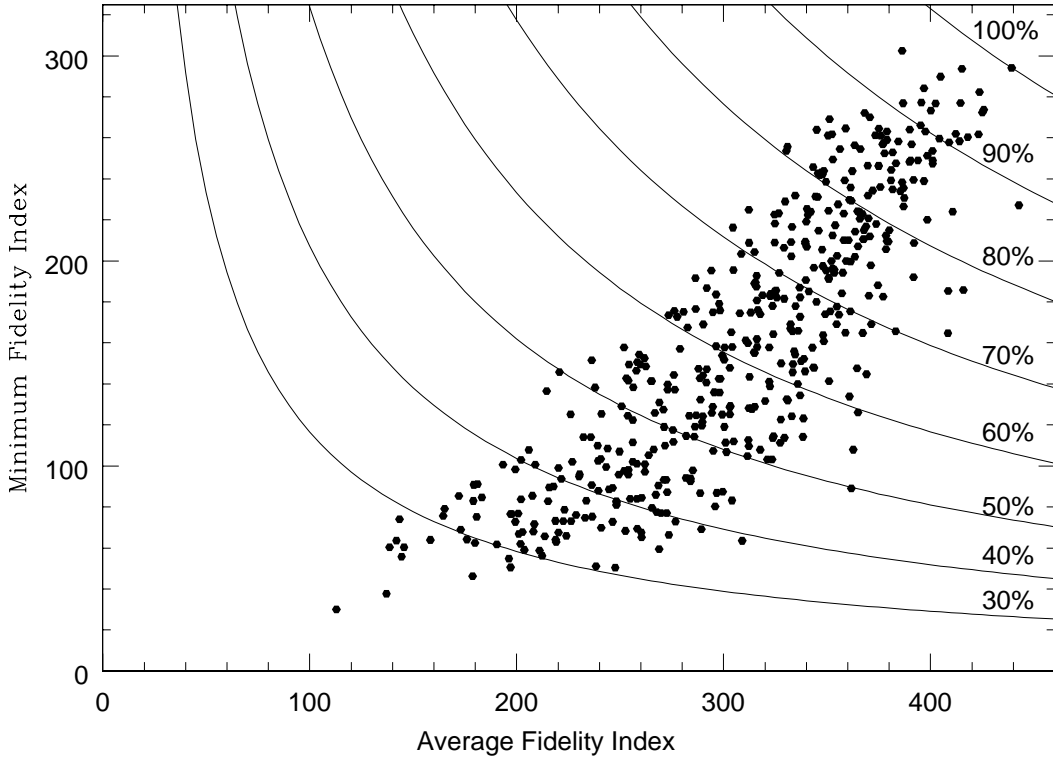


Fig. 7.— Average and Minimum Fidelity Indices for each potential LWIA array configuration.

other configurations with FOM nearly as high. The 20 “best” configurations are listed in Table 2.

To determine the three best outlier sites to develop first, we consider the best 10 of the configurations listed in Table 2. First, we note that only three of the “top 10” contain the site VS. The site VS is 7-8 miles away from any known fiber connection (Dickel et al. 2007). Though it is possible to install a fiber link, this is expensive. It might be worth the expense if this site were essential for high image fidelity, but being in only three of the top 10, this expense does not seem worthwhile. Therefore, we will avoid this site and the arrays that include it. That eliminates configurations 1, 2 and 6. Of the remaining seven best configurations, HS is the only site that is in all of them. Therefore HS should be selected. The next most frequent sites are PT, SV and HM, which are each in six of the remaining seven configurations. The PT site will be somewhat difficult to develop because it requires  $\sim 3$  miles of fiber to be installed. Further, that location already contains the Pie Town VLBA antenna which has a 74 MHz dipole and is connected by fiber to the VLA. To maximize the science that can be done with LWA1+, it would be best to develop other sites at that stage, and therefore we set aside PT for now. The site SV is at the UNM Field Station in the Sevilleta National Wildlife Refuge, and this site will not require the same land acquisition process as the others. Therefore, while it is likely we will eventually use this site, we set it aside for now also. That leaves HM, which we choose to select. With one more site to select, we consider

the next most frequently occurring sites, BH and EA, which are each in five of the remaining seven top-10 configurations. Because BH is probably too long of a baseline for the LWA1+, we select EA instead. This also makes sense as the combination of HS, HM and EA appears in configurations ranked 3, 4, 5 and 8 in Table 2 which are four of the top five array configurations that do not include VS. Therefore, including the site in the core, we conclude that the four best sites to begin development are NA, HS, HM and EA.

## REFERENCES

- A. Cohen, “A Potential Array Configuration for the LWA” Long Wavelength Array Memo #55, September 29, 2006
- A. Cohen, T. Clarke & J. Lazio “Early Science from the LWA Phase II: A Target List”, Long Wavelength Array Memo #80, February 12, 2007.
- J. Dickel, P. Crane, and A. Cohen, “More Sites for the LWA South Circle”, Long Wavelength Array Memo #99, September 3, 2007
- L. Kogan and A. Cohen, “Optimization of the LWA Antenna Station Configuration Minimizing Side Lobes”, Long Wavelength Array Memo #21, May 4, 2005
- G. Taylor et al. “LWA Overview”, Long Wavelength Array Memo #56, September 22, 2006.
- G. Taylor, P. Crane, F. Owen, J. Dickel, and W. Lucero, “A First Look at Sites for the LWA”, Long Wavelength Array Memo #62, November 13, 2006
- G. Taylor, A. Cohen, P. Crane, J. Dickel, and W. Lucero, “More Sites for the LWA: Sevilleta, Pie Town, Horse Springs, and Parts West”, Long Wavelength Array Memo #97, August 7, 2007
- G. Taylor, “LWA Data Communications - The Sneakernet Option” Long Wavelength Array Memo #110, November 30, 2007

Table 1: List of potential outlier LWIA station sites.

Name	Code	Long.	Lat.	Notes
Alamosa Creek	AC	−107.33°	33.30°	0.5 mile down from CO26, off of US25
Mule Creek	MC	−108.85°	33.12°	About 2 miles down Rt 78 off Rt 180
San Juan	SJ	−107.93°	32.79°	Near merger of Rt61N with Rt 152W,
VLA	VL	−107.63°	34.07°	Near VLA center (LWDA site)
Alegres Mountain	AM	−108.14°	34.21°	South of Pie Town
Black Hill	BH	−107.19°	33.57°	Off Rt 1, about 1.5 miles west of US25
East Arm	EA	−107.48°	34.03°	Off of the VLA east arm
Horse Mountain	HM	−108.00°	34.01°	Due East of Horse Mountain on NM12
Horse Springs	HS	−108.32°	33.89°	Probable Phase I station
Magdalena	MA	−107.17°	34.14°	few km north of Magdalena on NM169
Pie Town	PT	−108.15°	34.35°	Pie Town EVLA/VLBA site
Rock Springs Canyon	RC	−107.33°	34.03°	About 7 miles south of Magdalena
Sevilleta	SV	−106.90°	34.36°	In Sevilleta NWR at UNM Field Station
Twin Peaks	TP	−107.67°	34.13°	10 km east of Datil on US60
VLA South	VS	−107.66°	33.96°	8km south of VLA center on NM52

Table 2: List of LWIA configurations with the best figures of merit (FOM).

Rank	Fixed Sites				Chosen Sites						$FI_{min}$	$FI_{ave}$	FOM
1	AC	MC	SJ	VL	BH	HS	MA	RC	SV	VS	294.23	439.16	359.46
2	AC	MC	SJ	VL	BH	EA	HS	MA	SV	VS	293.64	415.18	349.16
3	AC	MC	SJ	VL	EA	HM	HS	PT	RC	SV	282.39	423.61	345.86
4	AC	MC	SJ	VL	BH	EA	HM	HS	PT	SV	289.85	404.85	342.56
5	AC	MC	SJ	VL	BH	EA	HM	HS	MA	PT	302.43	386.31	341.81
6	AC	MC	SJ	VL	BH	HM	HS	MA	SV	VS	273.69	425.73	341.35
7	AC	MC	SJ	VL	BH	HM	HS	MA	RC	SV	272.39	425.06	340.27
8	AC	MC	SJ	VL	EA	HM	HS	MA	PT	SV	277.04	414.48	338.86
9	AC	MC	SJ	VL	BH	EA	HS	MA	PT	SV	284.21	396.86	335.84
10	AC	MC	SJ	VL	BH	HM	HS	PT	RC	SV	276.78	402.44	333.75
11	AC	MC	SJ	VL	HS	MA	PT	RC	SV	VS	261.75	423.22	332.83
12	AC	MC	SJ	VL	BH	HS	MA	PT	RC	SV	277.21	395.54	331.13
13	AC	MC	SJ	VL	BH	HS	MA	PT	SV	VS	273.28	400.13	330.68
14	AC	MC	SJ	VL	BH	EA	HS	MA	RC	SV	260.45	418.00	329.95
15	AC	MC	SJ	VL	EA	HS	PT	RC	SV	VS	261.90	412.17	328.55
16	AC	MC	SJ	VL	BH	HM	HS	MA	PT	SV	276.91	386.72	327.24
17	AC	MC	SJ	VL	HM	HS	MA	PT	RC	SV	258.38	414.01	327.07
18	AC	MC	SJ	VL	BH	HM	HS	PT	SV	VS	257.76	409.01	324.69
19	AC	MC	SJ	VL	BH	HS	MA	RC	SV	TP	266.10	395.27	324.31
20	AC	MC	SJ	VL	BH	EA	HM	HS	RC	SV	259.59	404.25	323.94